In silico investigation of ligand-regulated palladium-catalysed formic acid dehydrative decomposition under acidic conditions

Chaoren Shen,*[ac] Kaiwu Dong,[a] Zhihong Wei[b] and Xinxin Tian*[b]

[a] Chang-Kung Chuang Institute, Shanghai Key Laboratory of Green Chemistry and Chemical Processes, School of Chemistry and Molecular Engineering, East China Normal University, Shanghai 200062 P. R. China. E-mail: shenchaoren@gmail.com

[b] Institute of Molecular Science, Key Laboratory of Materials for Energy Conversion and Storage of Shanxi Province, Shanxi University, Taiyuan 030006, P. R. China. E-mail: tianxx@sxu.edu.cn

[c] State Key Laboratory for Oxo Synthesis and Selective Oxidation (OSSO), Suzhou Research Institute of LICP, Lanzhou Institute of Chemical Physics (LICP), Chinese Academy of Sciences (CAS), Lanzhou 730000, China

Introduction

Carbonylation reactions constitute a potent tool to manufacture carboxylic acids and their derivatives both in industry and academic organic synthesis.[1-7] In general, the proceeding of carbonylation requires the use of toxic carbon monoxide, which thus usually demands certified high pressure reaction vessels.[8] Therefore, developing non-gaseous CO surrogate for conducting safe and facile-operation carbonylation with stoichiometric amount of CO in common Pyrex glass vessels (e.g., the two-chamber reactor[8] and sealed glass tube) is an important and ongoing research topic in the realm of homogenous catalysis.[9-15] Among these established CO surrogates, formic acid and its derivatives is one kind of versatile atom-economic C1 source. Different to the decomposition of formic ester or *N*-formyl imides releasing CO in the basic conditions for the carbonylation of aryl or alkyl halides,[16-18] the dehydrative decomposition of HCOOH to CO generally depends on the Morgan reaction using excess strong mineral acid (e.g., excess high-concentration sulfuric acid),[19] which is incompatible to the conditions for most of transition-metal catalysed carbonylation reactions. Moreover, undesired dehydrogenation of HCOOH to CO_2 and H_2, which is more thermodynamically favoured, can facilely occur in the presence of various homogenous transition-metal complex catalysts or heterogeneous catalysts and lead to the reduction of unsaturated bonds.[20] Thus, to avoid this side reaction, acetic anhydride has to be added as the activator for in-situ generating the more active CO source mixed anhydride.[21-24] In 2018, Beller and co-workers achieved the selective CO generation directly from HCOOH under acidic condition by a palladium-catalysed system with bidentate tertiary phosphine ligand bearing pyridyl substituents (py^{t}bpx), which was derived from 1,2-bis(di-*tert*-butylphosphino) methylbenzene (d^{t}pbx) (Figure 1).[25] The utility of this catalytic system in the autoclave-free hydrocarbonylation of all kinds of alkenes was also demonstrated.[25]

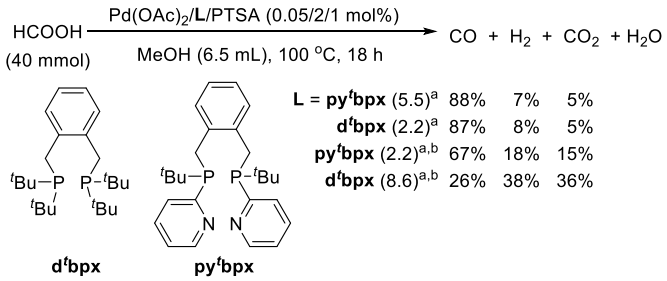

Figure 1. The ligand-regulated palladium-catalysed selective decomposition of HCOOH to CO. PTSA = *para*-toluenesulfonic acid.[25] [a]Molar percentage of gaseous products and in paratheses are total pressure (unit: bar) after reaction. [b]Without adding PTSA.

The experimental investigation by Beller *et al.* disclosed that the activity and selectivity of Pd catalyst to the HCOOH dehydration was regulated by both the ligand and the acid promoter (Figure 1). The ligand py^{t}bpx resulted from replacing two tetra-butyl substituents in d^{t}bpx with 2-pyridyl groups exhibited significantly higher CO selectivity than the original d^{t}bpx ligand (67% *vs*. 26%). Adding catalytic amount of *para*-toluenesulfonic acid (PTSA) can improved the CO selectivity (88% and 87%, respectively). Meanwhile, the activity towards dehydration using Pd-py^{t}bpx complex is considerably increased (5.5 bar *vs*. 2.2 bar) and higher than that of Pd-d^{t}bpx complex (more detailed results see Figure 1 of ref. 25). These results indicated the importance of "built-in base" (i.e., 2-pyridyl group) in enhancing the activity and selectivity of palladium catalyst.[26] Since the plausibility of in-situ generated methyl formate acting as CO-releasing agent has been experimentally ruled out[25] (details see Scheme 4 and S1 of ref. 25), we intended to elucidate the role of acid promoter and basic 2-pyridyl group of the ligand in palladium-catalysed formic acid dehydrative decomposition. By density functional theory-based computation, the difference between the Pd-py^{t}bpx and Pd-d^{t}bpx catalysts on the mechanism of formic acid dehydration to CO was revealed.

Computational method

All DFT calculations were performed using Gaussian 16 program.[27] Considering the applicability of meta-generalized gradient approximation (meta-GGA) functional M06[28] on homogeneous organometallic thermochemistry,[29] the M06 functional in conjugation with the def2-SVP basis set[30] was used for structure optimization. Corresponding frequency calculation using the same method was done to characterize the nature of the optimized structures; i.e., energy minimums without imaginary frequencies or transition states with only one imaginary frequency. Intrinsic reaction coordinate (IRC) was used to check the imaginary model that connects the initial and the final states. In addition, we used M06 in conjugation with the def2-TZVP basis set to conduct the self-consistent reaction field (SCRF) single-point calculations based on the M06/def2SVP-optimized geometries by using the SMD solvation model[31] and methanol as solvent to Gibbs free energies (M06-SCRF/def2-TZVP//M06/def2-SVP). The thermal corrections to Gibbs free energy at 373 K calculated by the Shermo program[32] were added to the total electronic energies from the SCRF single-point energy calculations. The corrected Gibbs free energy (ΔG) at 373 K were therefore used in the following discussion and comparison.

Results and discussion

HCOOH dehydration by Pd-py^{t}bpx or Pd-d^{t}bpx (paths A-D)

Experimental results have demonstrated that the presence of PTSA is critical to the activity and selectivity of Pd-catalysed dehydration of HCOOH.[25] Thus, two sets of mechanism with or without the aid of PTSA promoter were therefore considered for this process. A previous study has revealed that the nitrogen atom of the pyridyl ring has a higher proton affinity than the palladium atom in the acidic conditions,[26] similar trend is also found in this study. Therefore, the cationic Pd^0-py^{t}bpx complex **1-py^{t}bpx** bearing protonated pyridyl group is regarded as the active species for py^{t}bpx ligand, while the zero-valent palladium complex is chosen as the active species for d^{t}bpx ligand.

Fig. 2 illustrated the two plausible paths for HCOOH dehydration to CO catalysed by the palladium catalyst of py^{t}bpx (path **A** and **B**). Path **A** starts from the C-H activation of HCOOH by **1-py^{t}bpx** (HCOOH + **1-py^{t}bpx** → **2-py^{t}bpx** via **TS1-py^{t}bpx**) followed by the intramolecular dehydration facilitated by the pyridinium group (**2-py^{t}bpx** → **3-py^{t}bpx** + H_2O via **TS2-py^{t}bpx**). The first step is endergonic by 10.3 kcal/mol, with a barrier of 12.3 kcal/mol. The generated **2-py^{t}bpx** has an intramolecular hydrogen-bonding between the OH of COOH group and the proton attaching to the nitrogen atom of pyridyl group. The combination of OH and (N-)H and subsequent delivering one H_2O molecule has low barrier of 11.6 kcal/mol and is highly exergonic by 17.6 kcal/mol. Afterwards, the carbonyl palladium hydride complex **3-py^{t}bpx** can directly release CO with the formation of palladium hydride complex **4b-py^{t}bpx** followed by the direct hydrogen migration of **4b-py^{t}bpx** to regenerate **1-py^{t}bpx** via **TS3b-py^{t}bpx**. As shown in Fig. 2, the decarbonylation process is highly endergonic by 29.7 kcal/mol, but the hydrogen migration is almost barrierless. Considering the co-existence of PTSA, HCOOH and CH_3OH in the catalytic system, PTSA-, HCOOH- or CH_3OH-assisted hydrogen migration processes are investigated. It is found that although the ligand exchange with these three species is all endergonic, the three intermediates **4-py^{t}bpx**, **4a-py^{t}bpx** and **4c-py^{t}bpx** are all thermodynamically more stable than the **4b-py^{t}bpx** (1.5, 4.1, 4.6 vs. 22.4 kcal/mol). And the apparent Gibbs free energies of **TS3-py^{t}bpx** and **TS3a-py^{t}bpx** are lower than that of **TS3b-py^{t}bpx** (15.5, 16.1 vs. 20.3 kcal/mol), while the Gibbs free energy of **TS3c-py^{t}bpx** is much higher than that of **TS3b-py^{t}bpx** (34.3 vs. 20.3 kcal/mol). Therefore, we can deduce that PTSA- and HCOOH-assisted hydrogen migration processes are both possible. Since the following three reasons: i) the intermediate **4-py^{t}bpx** is more stable than **4a-py^{t}bpx** by 2.6 kcal/mol; ii) the Gibbs free energy of **TS3-py^{t}bpx** is 0.6 kcal/mol lower than that of **TS3a-py^{t}bpx**; iii) the *N*-protonation of ligand's pyridyl group in **3-py^{t}bpx** by PTSA is exothermic, while the corresponding protonation by less-acidic HCOOH is endothermic (more details see Fig. S1 in ESI), the PTSA-aid regeneration of **1-py^{t}bpx** is more facile than the corresponding process with HCOOH.

Path **B** also starts from the C-H activation of HCOOH by **1-py^{t}bpx** (HCOOH + **1-py^{t}bpx** → **2a-py^{t}bpx** via **TS1a-py^{t}bpx**). Differently, the intramolecular hydrogen-bonding in **TS1a-py^{t}bpx** and **2a-py^{t}bpx** lies between the oxygen atom of carbonyl group and the H-N moiety of pyridinium group. When **2a-py^{t}bpx** undergoes the intermolecular dehydration to **3a-py^{t}bpx** facilitated by PTSA or HCOOH as the proton shuttle respectively via **TS2a-py^{t}bpx** and **TS2b-py^{t}bpx** both containing eight-membered proton transfer ring or **TS2d-py^{t}bpx** and **TS2e-py^{t}bpx** both containing six-membered proton transfer ring, the corresponding energy barriers are high as 46.1, 39.0, 49.5 and 48.3 kcal/mol. The afforded H_2O comes from the combination of OH group of COOH and the proton of acid, while the hydrogen atom binding to Pd centre is transferred to the oxygen terminal of acid. In the absence of both PTSA and HCOOH, the subsequent intramolecular

dehydration of **2a-py^{t}bpx** squeezing out one H_2O molecule via **TS2c-py^{t}bpx** also needs to surmount the energy barrier of high as 39.9 kcal/mol. And the formed H_2O comes from the combination between the OH group of COOH and the H atom connecting to Pd. Finally, **1-py^{t}bpx** is regenerated from the decarbonylation of **3a-py^{t}bpx**, which is strongly endothermic by 19.8 kcal/mol. Whether the acid promoter attends or not, the high free energy for the transition state of dehydration is obviously disadvantageous to the reaction proceeding along path **B**.

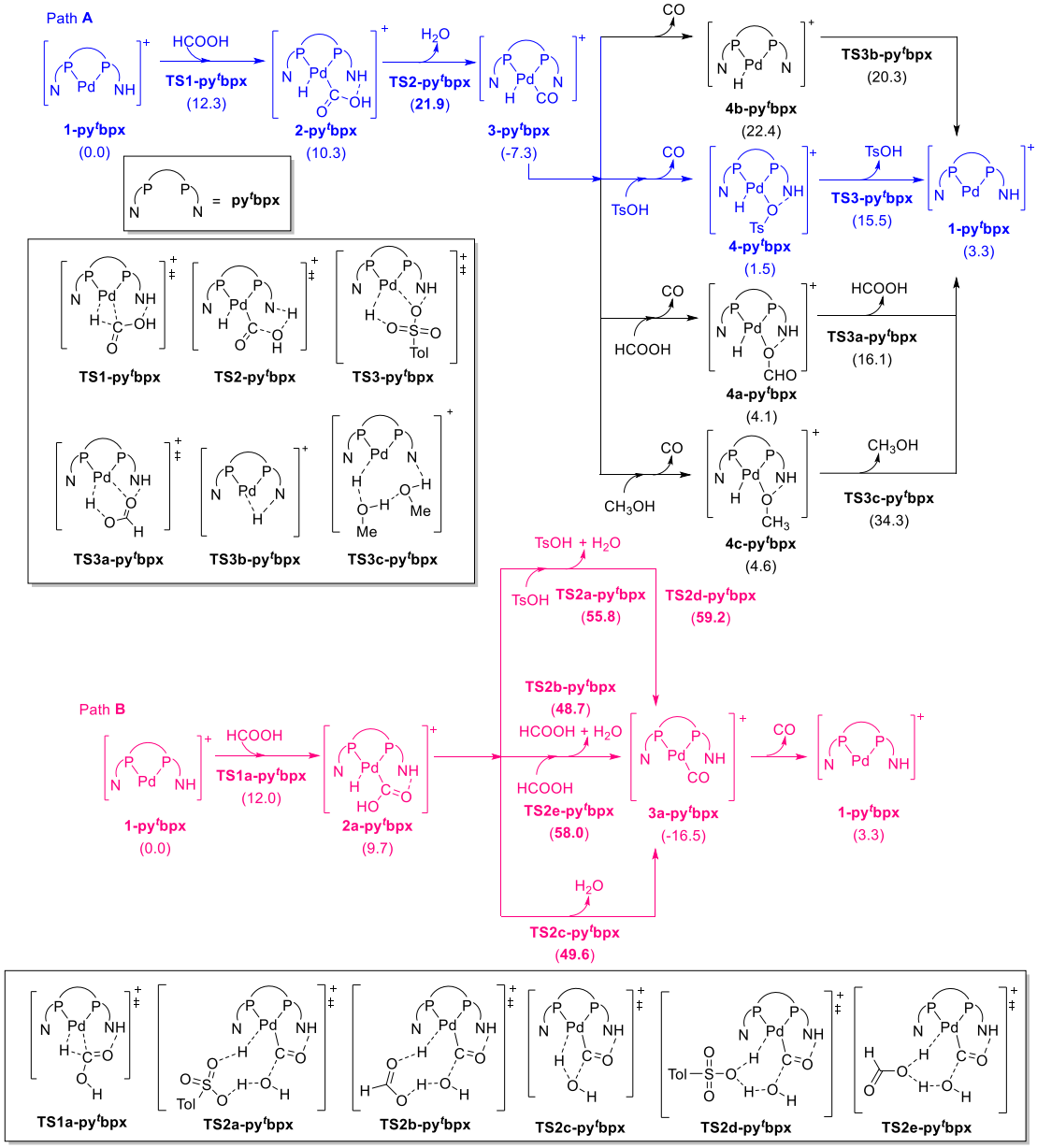

The obtained free-energy results about path **A** and **B** revealed the dehydration step (**2-py^{t}bpx** → **TS2-py^{t}bpx** and **2a-py^{t}bpx** → **TS2a-py^{t}bpx**) is the rate-degerming step in both paths. However, the free energy of **TS2-py^{t}bpx** is evidently much lower than that of **TS2a-py^{t}bpx** (21.9 vs. 48.7 kcal/mol). Suggesting that the protonated pyridyl group, which is known as "built-in base" group, can drastically reduce the apparent activation energy of HCOOH dehydration to CO by contributing its own proton. Furthermore, PTSA can considerably promote the regeneration of active species **1-py^{t}bpx**. Such outcomes indicate that adding PTSA can effectively relieve the hindrance to the regeneration of active species **1-py^{t}bpx** during the dehydration.

Fig. 3 displays the two plausible paths (path **C** and **D**) for HCOOH dehydration catalysed by the palladium catalyst of d^{t}bpx (**1-d^{t}bpx**). Similar to the dehydration by Pd-py^{t}bpx, both path **C** and **D** are also initiated from the C-H activation of HCOOH with **1-py^{t}bpx** (HCOOH + **1-d^{t}bpx** → **2-d^{t}bpx** via **TS1-d^{t}bpx**). The process is endergonic by 12.1 kcal/mol, with a barrier of 14.9 kcal/mol. The further transformation of **2-d^{t}bpx** has two alternatives: i) the acid-facilitated intermolecular dehydration to the carbonyl palladium hydride intermediate **3-d^{t}bpx** (path **C**); ii) the acid-promoted intermolecular dehydration or acid-absent intramolecular dehydration to the carbonyl palladium intermediate **3a-d^{t}bpx** (path **D**).

For path **C**, the PTSA-mediated intermolecular dehydration via **TS2-d^{t}bpx** exhibited significantly lower energy barrier than the HCOOH-mediated process via **TS2a-d^{t}bpx** (11.7 vs. 17.6 kcal/mol). The former process to **3-d^{t}bpx** is much more exothermic than the latter one (-30.6 vs. -14.8 kcal/mol). Thus, the transformation from **2-d^{t}bpx** to **3-d^{t}bpx** via **TS2-d^{t}bpx** is both kinetically and thermodynamically more favoured. For the PTSA- and HCOOH-attended intermolecular dehydration of **2-d^{t}bpx**, we also obtained the transition states **TS2e-d^{t}bpx and TS2f-d^{t}bpx** bearing six-membered ring structure for transferring proton from the acid onto the OH group. But both have much higher free energy than **TS2-d^{t}bpx** and **TS2a-d^{t}bpx**, respectively (details see Fig. S2 in ESI). Intermediate **4-d^{t}bpx** generated from the ligand exchange between carbonyl of **3-d^{t}bpx** and free *para*-toluenesulfonate anion is also more stable than **4a-d^{t}bpx** afforded from the ligand exchange between carbonyl ligand of **3-d^{t}bpx** and free formate anion. In the final step for regenerating **1-dtbpx**, the location of **TS3-d^{t}bpx** on the free energy surface is 2.8 kcal/mol lower than that of **TS3a-d^{t}bpx**. In path **D**, the intermolecular dehydration to **3a-d^{t}bpx** with the mediation of PTSA or HCOOH as proton shuttle via **TS2b-d^{t}bpx** and **TS2c-d^{t}bpx** both bearing eight-membered proton transfer chain requires to overcome the energy barrier of 13.8 or 18.7 kcal/mol. In comparison, the acid-absent intramolecular dehydration of **2-d^{t}bpx** to **3a-d^{t}bpx** via **TS2d-d^{t}bpx** requires to overcome the energy barrier of high as 37.8 kcal/mol. Moreover, the decarbonylation of **3a-d^{t}bpx** to regenerate **1-d^{t}bpx** and produce CO gas is endoergic by 15.3 kcal/mol. Although, the acid-mediated intermolecular dehydration in path **D** has moderate energy barrier, the lower free energy of **TS2-d^{t}bpx** than **TS2b-d^{t}bpx** by 2.1 kcal/mol suggests that PTSA-mediated path **C** is more advantageous than path **D** that also requiring the mediation of PTSA .
In Scheme 1, the solvated free-energy changes of path **A** for **py^{t}bpx** ligand and path **C** for **d^{t}bpx** ligand are compared. The lower free energy of **TS2-py^{t}bpx** than **TS2-d^{t}bpx** by 1.9 kcal/mol clearly manifests that the intramolecular dehydration by the protonated "built-in base" in py^{t}bpx ligand validly improves the catalytic efficiency of palladium catalyst in the dehydration of HCOOH to CO. Moreover, the lower free energy of **TS1-py^{t}bpx** than **TS1-d^{t}bpx** by 2.6 kcal/mol discloses that the presence of hydrogen-bonding interaction between HCOOH and the protonated py^{t}bpx ligand significantly mitigates the energy barrier for the C-H bond cleavage of HCOOH and stabilizes the intermediate **2-py^{t}bpx**.

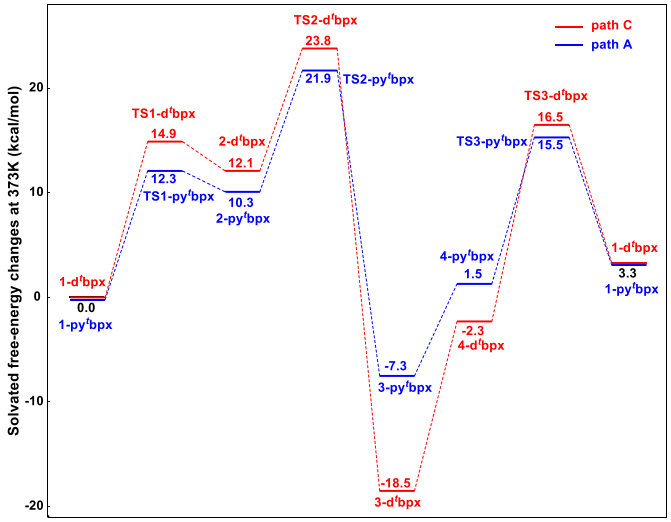

Scheme 1 The solvated free-energy changes of path **A** and **C** at 373 K.

HCOOH dehydrogenation by Pd-py^{t}bpx or Pd-d^{t}bpx (path E and F)

As the side reaction during the dehydration of HCOOH, the HCOOH dehydrogenation to H_2 and CO_2 by Pd-py^{t}bpx (path **E**) or Pd-d^{t}bpx (path **F**) demonstrated in Fig. 4 undergoes a two-step process starting from the C-H activation of HCOOH by **1-py^{t}bpx** or **1-d^{t}bpx** followed by the dehydrogenative decomposition of **2a-py^{t}bpx** and **2-d^{t}bpx** yielding H_2 and CO_2. Similar to the scenario in the dehydration, the dehydrogenation of **2a-py^{t}bpx** and **2-d^{t}bpx** also have three different channels: PTSA- or HCOOH-mediated intermolecular dehydrogenation correspondingly via **TS4a** and **TS4b**, as well as the direct intramolecular dehydrogenation via **TS4**. Different circumstance was exhibited on the catalysts of Pd-d^{t}bpx and Pd-py^{t}bpx. For Pd-d^{t}bpx, the free energy of **TS4b-py^{t}bpx** is about 2.2 kcal/mol lower than **TS4-py^{t}bpx** and **TS4a-py^{t}bpx**. The HCOOH-mediated dehydrogenation is more favoured. Meanwhile, for Pd-py^{t}bpx, the free energy of **TS4a-d^{t}bpx** is much lower than **TS4-d^{t}bpx** and **TS4b-d^{t}bpx**. The PTSA-mediated dehydrogenation is preferred. In path **E** and **F**, the intramolecular dehydrogenation of **2a-py^{t}bpx** and **2-d^{t}bpx** respectively via **TS4b-py^{t}bpx** and **TS4a-d^{t}bpx** is the rate-determining step with the energy barrier of 24.7 and 19.2 kcal/mol. The apparent activation energy for path **E** and **F** are high as 34.4 and 31.3 kcal/mol.

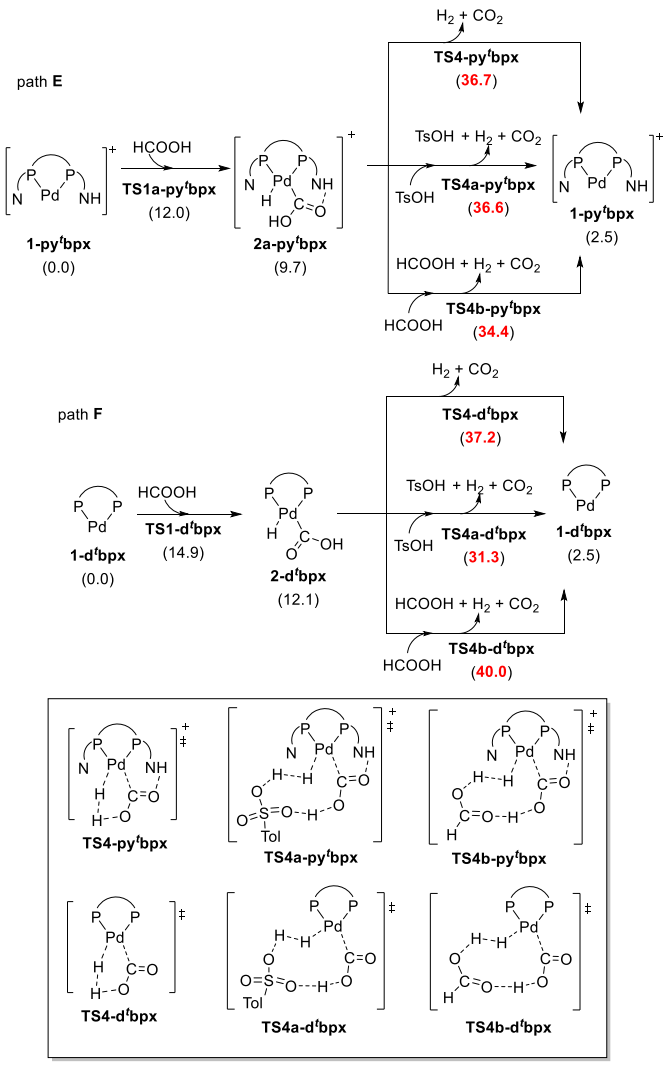

Figure 4 The dehydrogenation of HCOOH respectively catalysed by Pd/py^{t}bpx and Pd/d^{t}bpx (path **E** and **F**)

Comparing the energy profiles of four paths (path **A**, **C**, **E** and **F**) together in Scheme 2, we can see that although the reaction process of dehydrogenation has fewer elementary steps than dehydration, the PTSA-mediated dehydration of HCOOH catalysed by Pd-py^{t}bpx is obviously more favourable than the corresponding dehydrogenation, owing to the much lower apparent activation energy of path **A** than **E**. Such advantage is unaffected under the PTSA-free reaction conditions, since the dehydrogenation of **2a-py^{t}bpx** should be accomplished by HCOOH instead of PTSA (via **TS4b-py^{t}bpx** instead of **TS4a-py^{t}bpx**), which rationalizes the stable chemoselectivity to CO by Pd-py^{t}bpx under the PTSA-absent conditions. In sharp contrast to the observed remarkable stability of Pd-py^{t}bpx catalyst,[25,33,34] the catalyst of Pd-d^{t}bpx is always prone to decompose in either the absence or the presence of PTSA under heating conditions, which leads to the formation of Pd nanoparticles (i.e., Pd black).[34,35] Such distinction on stability is more obvious under the water-contained acidic conditions.[34,35] Since the dehydrogenation of HCOOH catalysed by palladium nanoparticle under low temperature is rather facile,[36-39] we infer that the dehydrogenation during the dehydration of HCOOH catalysed by Pd-d^{t}bpx is probably contributed by the palladium nanoparticle resulted from the degradation of Pd-d^{t}bpx catalyst. The palladium nanoparticles were also reported to exhibit somewhat both size- and morphology-dependent

dehydration activity.[40-42] Thus, the catalyst of Pd-d^{t}bpx fails to possess the stable chemoselectivity that comparable to Pd-py^{t}bpx.

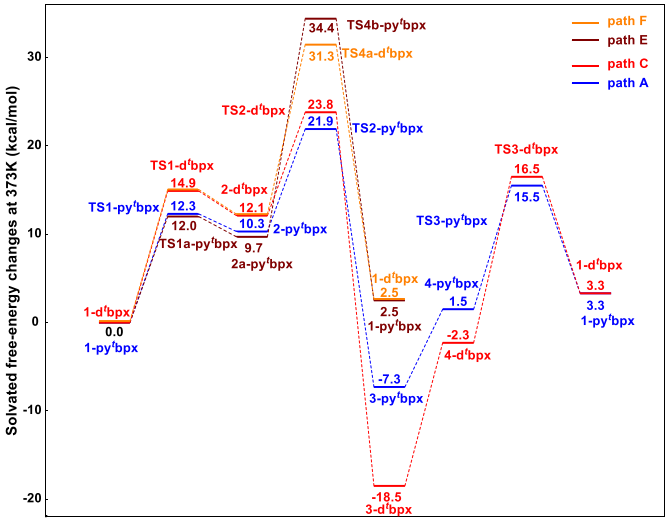

Scheme 2 The solvated free-energy changes of path **A**, **C** , **E** and **F** at 373 K.

Conclusions

In summary, the DFT-based computational survey unveils the role of "built-in base" and strong *para*-toluenesulfonic acid promoter in the dehydrative decomposition of HCOOH to CO catalysed by Pd-py^{t}bpx. The basic pyridyl group installed in the ligand of py^{t}bpx changes the mode of intermolecular dehydration aid by the acid promoter to the mode of intramolecular dehydration facilitated by the pyridinium group, which turns down the apparent activation energy of reaction. The participation of *para*-toluenesulfonic acid in the process of regenerating active Pd-py^{t}bpx catalyst promotes the proceeding of reaction.

Author Contributions

C. S.: writing original draft, investigation, formal analysis, methodology, visualization; X. T.: review & editing conceptualization, methodology, project administration; Z. W.: review & editing; K. D.: conceptualization, funding acquisition. All the authors discussed the results and contributed to the writing of the manuscript.

Conflicts of interest

There are no conflicts to declare.

Acknowledgements

C.S. and X.T. thank the financial supports from the National Natural Science Foundation of China (No. 21903049 for X.T., 21802151 for C.S.) Part of the calculations were performed at the Shanghai Supercomputer Centre and the Supercomputing Centre of Shanxi University.

Notes and references

1. R. Sang, Y. Hu, R. Razzaq, R. Jackstell, R. Franke and M. Beller, *Org. Chem. Front.,* 2021, **8**, 799-811.

2. Z. Yin, J.-X. Xu and X.-F. Wu, *ACS Catal.*, 2020, **10**, 6510-6531.

3. J.-B. Peng, F.-P. Wu and X.-F. Wu, *Chem. Rev.,* 2019, **119**, 2090-2127.

4. X.-F. Wu, X. Fang, L. Wu, R. Jackstell, H. Neumann and M. Beller, *Acc. Chem. Res.,* 2014, **47**, 1041-105.

5. X.-F. Wu, H. Neumann and M. Beller, *Chem. Rev.,* 2013, 113, 1-35.

6. J. Pospech, I. Fleischer, R. Franke, S. Buchholz and M. Beller, *Angew. Chem. Int. Ed.,* 2013, **52**,

2852-2872.
7. A. Brennführer, H. Neumann and M. Beller, *Angew. Chem. Int. Ed. Engl.,* 2009, **48**, 4114-33.
8. S. D. Friis, A. T. Lindhardt and T. Skrydstrup, *Acc. Chem. Res.* 2016, **49**, 594-605.
9. Z. Chen, L.-C. Wang and X.-F. Wu, *Chem. Commun.*, 2020, **56**, 6016-6030.
10. L. Wang, W. Sun and C. Liu, *Chin. J. Chem.,* 2018, **36**, 353-362.
11. H. Konishi, *Chem. Pharm. Bull.* 2018, **66**, 1-19.
12. P. Gautama and B. M. Bhanage, *Catal. Sci. Technol.*, 2015, **5**, 4663-4702.
13. L. Wu, Q. Liu, R. Jackstell and M. Beller, *Angew. Chem. Int. Ed.*, 2014, **53**, 6310-6320.
14. L. R. Odell, F. Russo and M. Larhed, *Synlett*, 2012, 685-698.
15. T. Morimoto and K. Kakiuchi, *Angew. Chem. Int. Ed.,* 2004, **43**, 5580-5588.
16. F. Ramirez-Vega*,* P. Laurent*,* J.-C. Clément and H. des Abbayes *J. Mol. Catal. A: Chem.*, 1995, **96**, 15-20.
17. T. Ueda, H. Konishi and K. Manabe, *Angew. Chem. Int. Ed.*, 2013, **52**, 8611-8615.
18. L.-B. Jiang, X. Qi and X.-F. Wu, *Tetrahedron Lett.*, 2016, **57**, 3368-3370.
19. (a) J. S. Morgan, *J. Chem. Soc., Trans.*, 1916, **109**, 274-283; (b) R. E. DeRight, *J. Am. Chem. Soc.*, 1933, **55**, 4761-4764; (c) G. Ciuhandu, A. Dumitreanu and Z. Simon, *J. Prakt. Chem.*, 1976, **318**, 202-206.
20. J. Guo, C. K. Yin, D. L. Zhong, Y. L. Wang, T. Qi, G. H. Liu, L. T. Shen, Q. S. Zhou, Z. H. Peng, H. Yao and X. B. Li, *ChemSusChem*, 2021, **14**, 2655-2681.
21. J. Hou, J.-H. Xie and Q.-L. Zhou, *Angew. Chem. Int. Ed.,* 2015, **54**, 6302-6305.
22. J. Dai, W. Ren, W. Chang, P. Zhang and Y. Shi, *Org. Chem. Front.*, 2016, **3**, 1131-1136.
23. W. Liu, W. Ren, J. Li, Y. Shi, W. Chang and Y. Shi, *Org. Lett.*, 2017, **19**, 1748-1751.
24. W. Ren, J. Chu, F. Sun, Y. Shi, *Org. Lett.*, 2019, **21**, 5967-5970.
25. R. Sang, P. Kucmierczyk, K. Dong, R. Franke, H. Neumann, R. Jackstell and M. Beller*, J. Am. Chem. Soc.*, 2018, **140**, 5217-5223.
26. K. Dong, R. Sang, Z. Wei, J. Liu, A. Spannenberg, H. Jiao, R. Franke and M. Beller, *Chem. Sci.*, 2018, **9**, 2510-2516.
27. M. J. Frisch, G. W. Trucks, H. B. Schlegel, G. E. Scuseria, M. A. Robb, J. R. Cheeseman, G. Scalmani, V. Barone, G. A. Petersson, H. Nakatsuji, X. Li, M. Caricato, A. V. Marenich, J. Bloino, B. G. Janesko, R. Gomperts, B. Mennucci, H. P. Hratchian, J. V. Ortiz, A. F. Izmaylov, J. L. Sonnenberg, D. Williams-Young, F. Ding, F. Lipparini, F. Egidi, J. Goings, B. Peng, A. Petrone, T. Henderson, D. Ranasinghe, V. G. Zakrzewski, J. Gao, N. Rega, G. Zheng, W. Liang, M. Hada, M. Ehara, K. Toyota, R. Fukuda, J. Hasegawa, M. Ishida, T. Nakajima, Y. Honda, O. Kitao, H. Nakai, T. Vreven, K. Throssell, J. A. Montgomery, Jr., J. E. Peralta, F. Ogliaro, M. J. Bearpark, J. J. Heyd, E. N. Brothers, K. N. Kudin, V. N. Staroverov, T. A. Keith, R. Kobayashi, J. Normand, K. Raghavachari, A. P. Rendell, J. C. Burant, S. S. Iyengar, J. Tomasi, M. Cossi, J. M. Millam, M. Klene, C. Adamo, R. Cammi, J. W. Ochterski, R. L. Martin, K. Morokuma, O. Farkas, J. B. Foresman, and D. J. Fox, Gaussian 16., Revision A.03.03, Gaussian, Inc., Wallingford C.T, 2016.
28. Y. Zhao and D. G. Truhlar, *Theor. Chem. Account.,* 2008, **120**, 215-241.
29. Y. Zhao and D. G. Truhlar, *Acc. Chem. Res.*, 2008, **41**, 157–167
30. F. Weigend and R. Ahlrichs, *Phys. Chem. Chem. Phys.* 2005, **7**, 3297-3305.
31. A. V. Marenich, C. J. Cramer and D. G. Truhlar, *J. Phys. Chem.* B 2009, **113**, 6378-6396.
32. T. Lu and Q. Chen, *Comput. Theor. Chem.*, 2021, **1200**, 113249.
33. R. Sang, P. Kucmierczyk, R. Dühren, R. Razzaq, K. Dong, J. Liu, R. Franke, R. Jackstell,

Angew. Chem. Int. Ed. 2019, **58**, 14365-14373
34. K. Dong, R. Sang, J. Liu, R. Razzaq, R. Franke, R. Jackstell and M. Beller, *Angew. Chem., Int. Ed.* 2017, **56**, 6203−6207.
35. J. Vondran, M. R. L. Furst, G. R. Eastham, Thomas Seidensticker and D. J. Cole-Hamilton, C*hem. Rev.*, 2021, **121**, 6610−6653
36. Q.-Y. Bi, J.-D. Lin, Y.-M. Liu, H.-Y. He, F.-Q. Huang and Y. Cao, *Angew. Chem. Int. Ed.*, 2016, **55**, 11849-11853.
37. H. J. Young and M. Chung, *App. Catal. B, Environ.*, 2017, **210**, 212-222.
38. Q. Wang, N. Tsumori, M. Kitta and Q. Xu, *ACS Catal.* 2018, **8**, 12, 12041-12045.
39. L. Di, J. Zhang, M. Craven, Y. Wang, H. Wang, X. Zhang, and X. Tu, *Catal. Sci. Technol.*, 2020, **10**, 6129-6138.
40. S. Jones, S. M. Fairclough, M. Gordon-Brown, W. Zheng, A. Kolpin, B. Pang, W. C. H. Kuo, J. M. Smith and S. C. E. Tsang, *Chem. Commun*., 2015, **51**, 46-49.
41. S. Zhang, B. Jiang, K. Jiang, and W.-B. Cai, *ACS Appl. Mater. Interfaces*, 2017, **9**, 24678-24687.
42. Y. Kim and D. H. Kim, *App. Catal. B: Environ.*, 2019, **244**, 684-693.